The American Journal of Human Genetics

Supplemental Data

RNASEH1 Mutations Impair mtDNA Replication and Cause Adult-Onset Mitochondrial Encephalomyopathy

Aurelio Reyes, Laura Melchionda, Alessia Nasca, Franco Carrara, Eleonora Lamantea, Alice Zanolini, Costanza Lamperti, Mingyan Fang, Jianguo Zhang, Dario Ronchi, Sara Bonato, Gigliola Fagiolari, Maurizio Moggio, Daniele Ghezzi, and Massimo Zeviani

Supplemental Case Reports

Subject 1

Subject 1 (S1) is a 42 year old male born after uncomplicated pregnancy and delivery, from healthy unrelated parents. He has two healthy daughters. His psychomotor development was normal. At 20 years of age he started complaining of muscle pain and at 21 he noticed eyelid ptosis associated with progressive ophthalmoplegia, occasional dysphagia, speech difficulties, and postural instability. At neurological examination he showed CPEO, dysarthria, dysphonia, wide-based gait, exercise intolerance with muscle cramps and weakness, particularly affecting the lower limbs. Neither hearing loss nor cardiac abnormalities nor diabetes were reported. Bilateral eyelid ptosis required surgery at the age of 32. At 36 he experienced recurrent episodes of ventilatory insufficiency including nocturnal dyspnoea and orthopnea; an acute episode required tracheostomy. He nevertheless recovered from this condition and later respiratory assessment disclosed only a mild restrictive deficit, without sleep apnoea, dyspnoea or orthopnea (average nocturnal oxygen saturation about 90%). ECG and Echocardiogram were normal. Laboratory tests showed high CK levels (400 U/L; normal values, n.v. <195) and mild lactate increase (2856 μmol/L; n.v. 580-2100). Brain MRI revealed moderate cerebellar and brain stem atrophy. A neurophysiologic assessment was performed: an Electromyography (EMG) showed mild motor demyelinating neuropathy prevalent in the lower limbs, eyelid and distal myopathic signs; Multimodal Evoked Potentials: multisystem CNS involvement with particularly altered Somatosensory evoked potentials (SEP) in the lower limbs.

A muscle biopsy showed numerous ragged-red and COX negative fibres. Respiratory chain analysis performed on muscle tissue showed partial reduction of complex I and IV activity; the same analysis did not show alteration when performed on S1 skin fibroblasts.

In the last few years, S1 experienced mild worsening of standing and gait stability, while muscle weakness and ventilatory impairment are stable.

Subject 2

Subject 2 (S2), a 46 year old man, is the second child of healthy non consanguineous parents. Family history was negative for neurological diseases; his motor development was normal and he had a regular scholastic course. He had no

neuromuscular abnormalities until 23 years of age, when he developed a progressive bilateral ptosis without diplopia. Neurological examination showed lateral and up gaze ophthalmoplegia, brisk reflexes with distal clonus and bilateral extensory plantar response. He referred fatigability, with no dyspnoea, dysphonia or dysphagia. The laboratory examination of plasma gave normal results with the only exception of increased lactate (30.8 mg/dl; n.v. 5.7-22 mg/dl). The EMG showed mild neurogenic signs; the EEG indicated generalized slow wave activity, with paroxysmal bilateral graphoelements, enhanced by hyperpnoea. An Echocardiogram (ECG) showed right bundle branch block pattern; fundus oculi and audiometry were normal. CSF investigation showed no pathological issues. MRI study was refused because of claustrophobia. Histological examination on biceps muscle biopsy displayed ragged red fibres (RRF) and absence of COX activity in several scattered fibres, many of which also showing intense SDH-positivity. Spectrophotometric analysis of MRC complex activities normalized to citrate synthase (CS) showed decreased cIV/CS ratio in muscle homogenate and in myoblasts (55% of control mean in both specimens), with partial reduction of cI+cIII/CS ratio (62%). Over the following 20 years, S2 experienced worsening of ocular movements and muscle weakness. At the latest neurological examination (45 years of age) he presented severe gait impairment, being now unable to walk long distance, needing a wheelchair. Progressive head drop, dysphagia and trunk weakness had ensued. He also presented decreased visual acuity (5/10 right, 2/10 left), a complete ophthalmoplegia and profound weakness of orbicular oris and oculi muscles leading to corneal lesions with neovascularization. Other features included hypotrophy of interossei and thenar eminence, moderate limb (MRC 3-4/5) and marked axial muscle weakness (MRC 2-3/5), with tendency to propulsion of head and trunk. Mild cerebellar signs in the upper limbs were present; tendon reflexes were decreased, sensory examination showed isolated impairment of discriminative perception. Visual evoked potentials were undetectable. Electroretinogram showed reduction in amplitude. The subject developed arterial hypertension without respiratory and cardiologic involvement.

Siblings S3-6

Subject 5 (S5) was born after uncomplicated pregnancy and delivery from healthy related parents. The same clinical phenotype was reported in three siblings (S3, S4, S6) while other four siblings were unaffected (Fig. 1a). She had two daughters and

one son, all healthy. At 45 years old she started complaining of eyelid ptosis and ophthalmoparesis. The symptoms worsened progressively and she started presenting dysphonia, dysphagia leading to significant weight loss, and walking difficulties. The clinical examination at 48 years showed CPEO with paraparetic gait associated with pyramidal signs, and increased deep tendon reflexes. Some cerebellar signs were noticed such as dysmetria and a positive Romberg sign. Cognitive impairment and motor slowing were present. A brain MRI showed cerebellar and cortical atrophy with hyper-intense lesions in the deep periventricular white matter. She did not report hearing loss. The EMG pattern showed diffuse, proximal neuropathy. Cardiologic assessment was normal (ECG) at 48 years of age. CK levels were reported as normal. A muscle biopsy performed at the age of 48 showed ragged-red and COX negative fibres. She died at the age of 63 years for a sudden cardiac event.

Her younger sister (S6), now aged 65, had a similar disease history. She started at 40 years presenting with CPEO associated with progressive gait instability, severe dysphagia and ventilatory impairment. A muscle biopsy performed at 40 years showed mitochondrial myopathy (ragged red and COX negative fibers). She is now wheelchair bound, receives nutrients through a percutaneous endoscopic gastrostomy (PEG) and needs ventilatory support (non-invasive ventilation, NIV) during the day and oxygen administration during the night.

A second sister (S4) died at 70 years because of respiratory failure and an older brother (S3) died at 60 years of unknown cause. Both were reported to have suffered of a similar condition with CPEO, dysphagia and respiratory impairment.

Figure S1: **Recombinant RNAseH1 protein purification and *in vitro* assay**

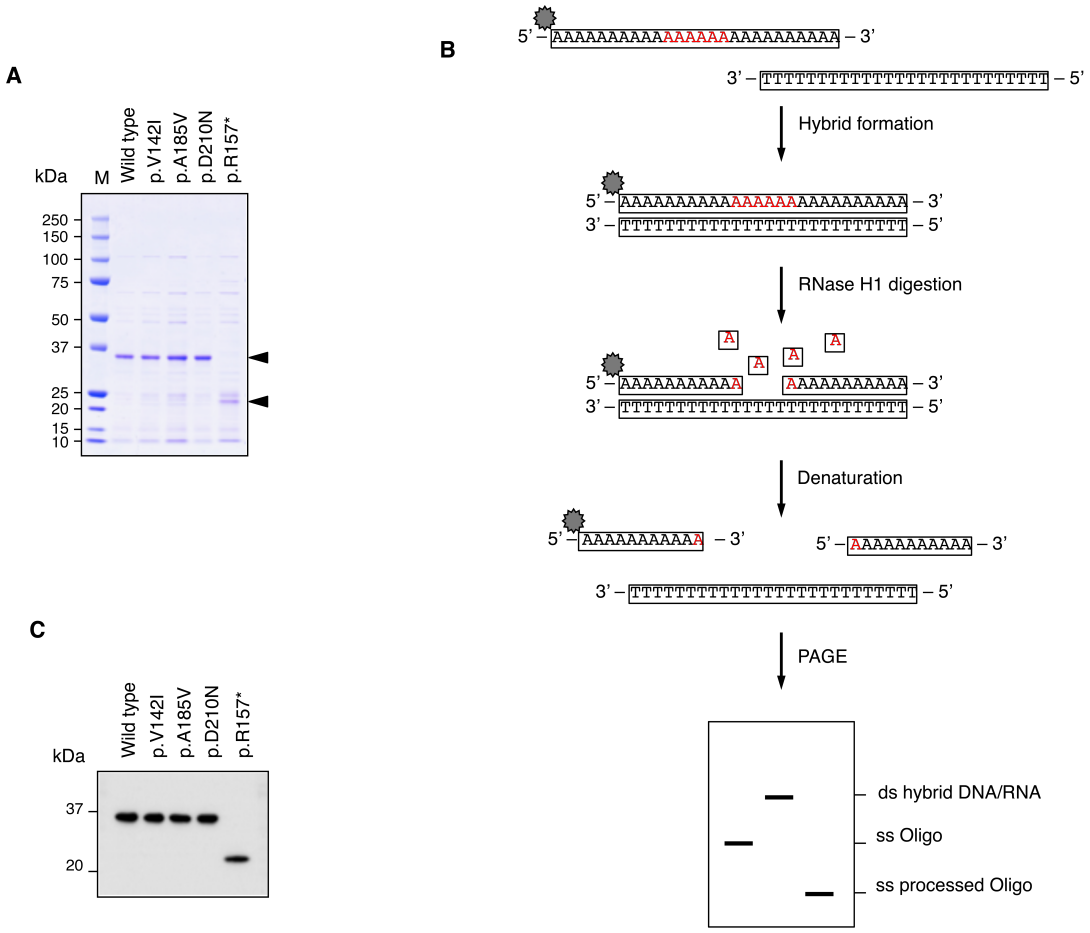

(A) SDS-PAGE gel stained with Coomassie Brilliant Blue showing the protein profile of eluted fractions with 400 mM imidazole from the affinity purification of wt and mutant HIS.RNASEH1.HIS. The most intense protein bands (marked with arrowheads) of ~37 and ~21 kDa correspond to the purified HIS.RNASEH1.HIS protein.

(B) In vitro assay for the measurement of RNAseH1 activity. A 5' end Cy5.5 fluorescently labelled chimeric oligo $dA_{10}A_6dA_{10}$ was hybridised to an oligo dT_{26} and incubated at 37ºC for 1h. In the presence of active RNAseH1, the RNA component of the heteroduplex is cleaved. Then, loading buffer containing formamide was added and samples boiled at 85ºC for 5 min, and then cooled on ice before loading onto 15% polyacrylamide gels in 1xTBE. This will produce a processed fragment of shorter length but still labelled at the 5' end and clearly distinguishable from the non-cleaved oligo used to form the heteroduplex. Control heteroduplex was not denatured before loading to avoid separation of the two strands and is loaded only as reference.

(**C**) The identity of the purified proteins was confirmed by Western blotting with anti-His antibody. These Western blots were also used as loading control for the normalization of the in vitro activity shown in **Figure 1C**.

Figure S2: ***RNASEH1* transcript levels**

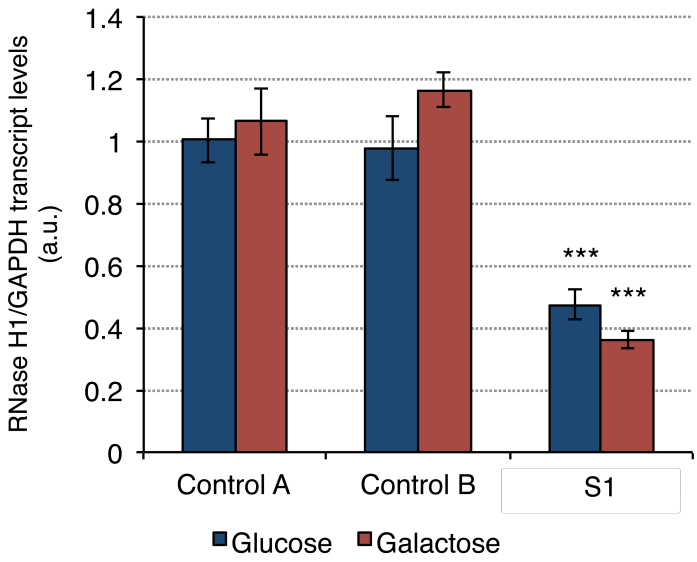

Transcript levels were investigated with Life Technologies Gene Expression Assay (Hs00268000_m1) and normalized to GAPDH (Hs02758991_g1). Cells were grown in either glucose or galactose for five days. ***$P < 0.001$; two-tailed Student's t test; $n = 2$; error bars = 1 s.d.

Figure S3: **Cell cycle analysis**

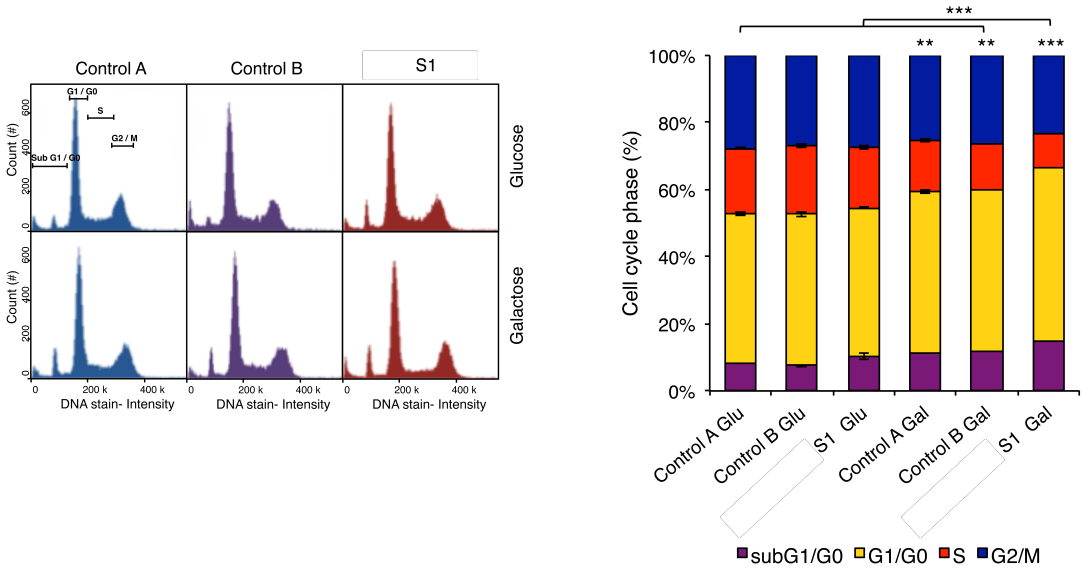

Control and mutant fibroblasts grown in glucose or galactose for five days were subjected to cell cycle analysis using propidium iodine (left). The proportion of cells in sub G1/G0, G1/G0, S and G2/M phases was scored for each sample (right). $^{**}P < 0.01$, $^{***}P < 0.001$; two-tailed Student's *t* test; $n = 4$; error bars = 1 s.d.

Figure S4: **Mitochondrial membrane potential**

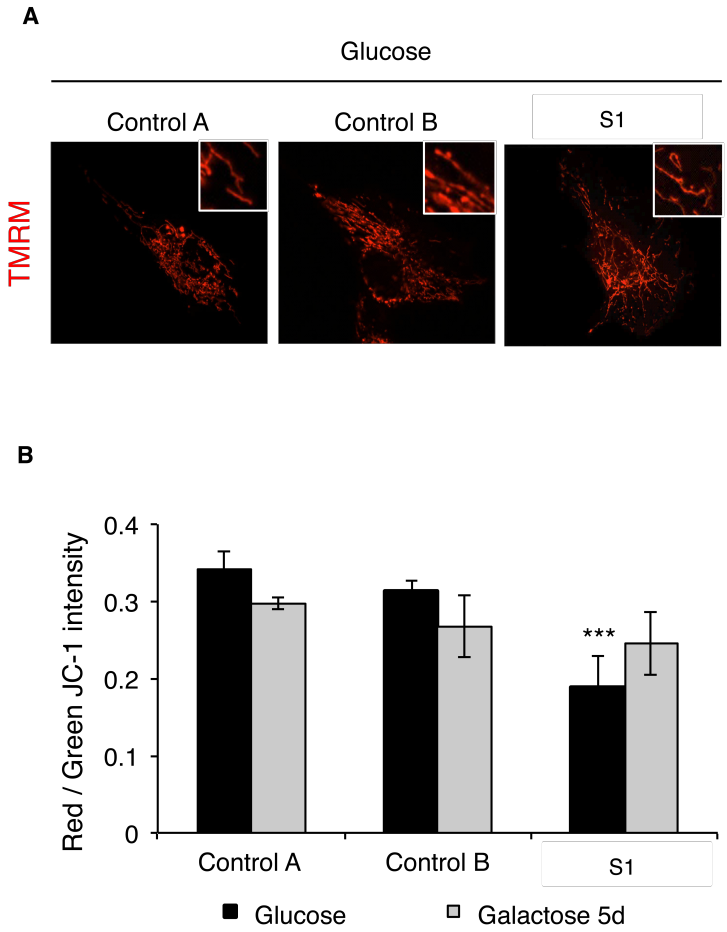

(A) TMRM staining of live cells grown in glucose for five days as shown in **Figure 2B** was indicative of lower membrane potential in mutant fibroblast. However, the low signal did not allow a proper comparison of the mitochondrial morphology. Therefore, the signal has been two-fold enhanced in the *RNASEH1* mutant fibroblasts in order to better appreciate the mitochondrial network. No significant difference compared to controls is observed.
(B) Quantification of mitochondrial membrane potential in fibroblasts grown in glucose or galactose for five days using JC-1 staining. The ratio of red to green JC-1 is plotted for the different samples as a measure of mitochondrial membrane potential. ***$P < 0.001$; two-tailed unpaired Student's t test; $n = 4$; error bars = 1 s.d.

Figure S5: **Nucleoid measurements**

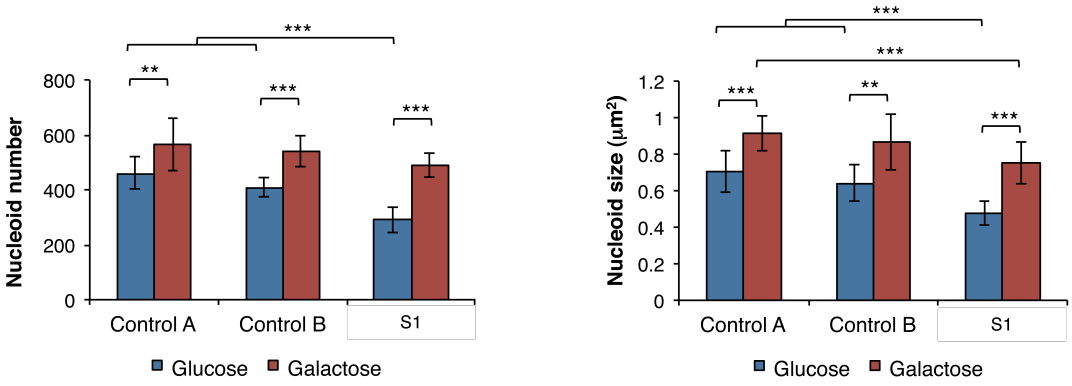

Nucleoid number (left) and size (right) were quantified in live cells grown in glucose or galactose for five days and stained with PicoGreen. Cells were imaged with a ZEISS ApoTome fluorescence microscope using a 40X immersion objective. Analysis was carried out using Particle Counting application available in ImageJ. $^{**}P < 0.01$; $^{***}P < 0.001$; two-tailed Student's *t* test; $n = 10$; error bars = 1 s.d.

Figure S6: **Mitochondrial DNA copy number**

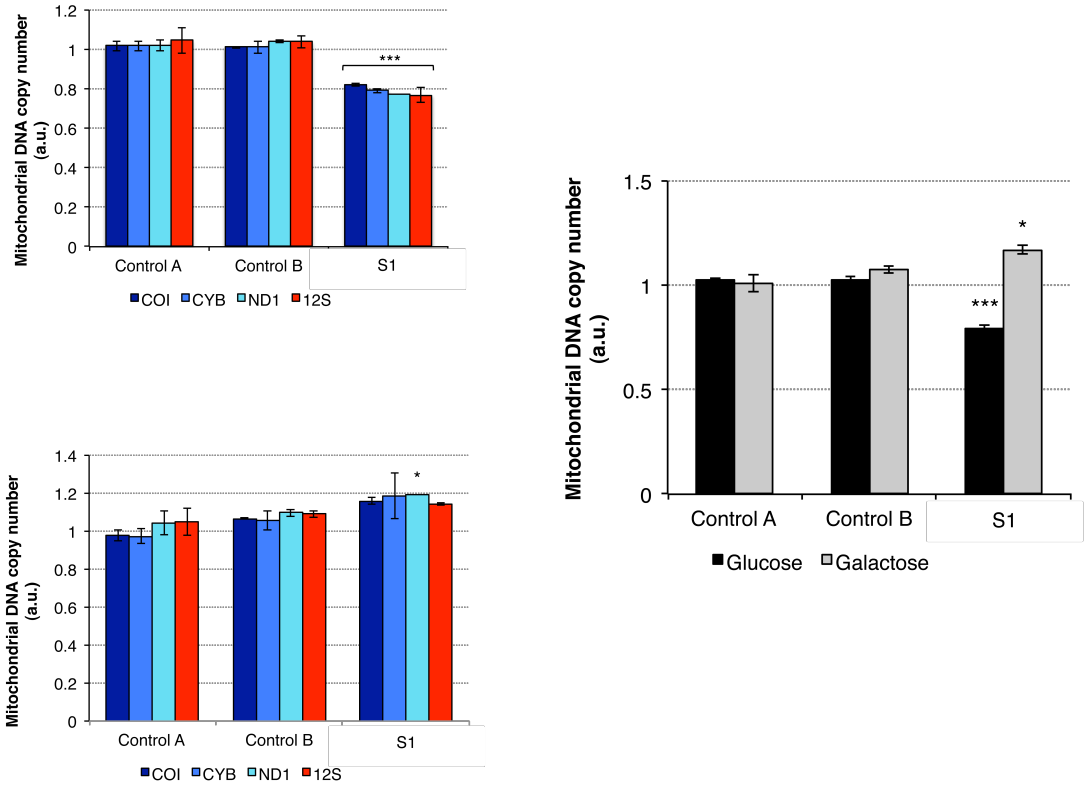

Relative mtDNA copy number was assessed in cells grown in glucose (top left) or galactose (bottom left) for five days by qPCR using Life Technologies Gene Expression Assays for four mitochondrial genes: COI (Hs02596864_g1), CYB (Hs02596867_s1), ND1 (Hs02596873_s1) and 12S rDNA (H202596859) and normalized to APP (Hs02339796_cn) levels. Control cells grown in glucose were arbitrarily chosen as reference and given value 1. Average of all four mitochondrial genes are shown on the right. *$P < 0.05$; ***$P < 0.001$; two-tailed unpaired Student's t test; $n = 4$; error bars = 1 s.d.

Figure S7: **Quantification of replication intermediates from 2D-AGE**

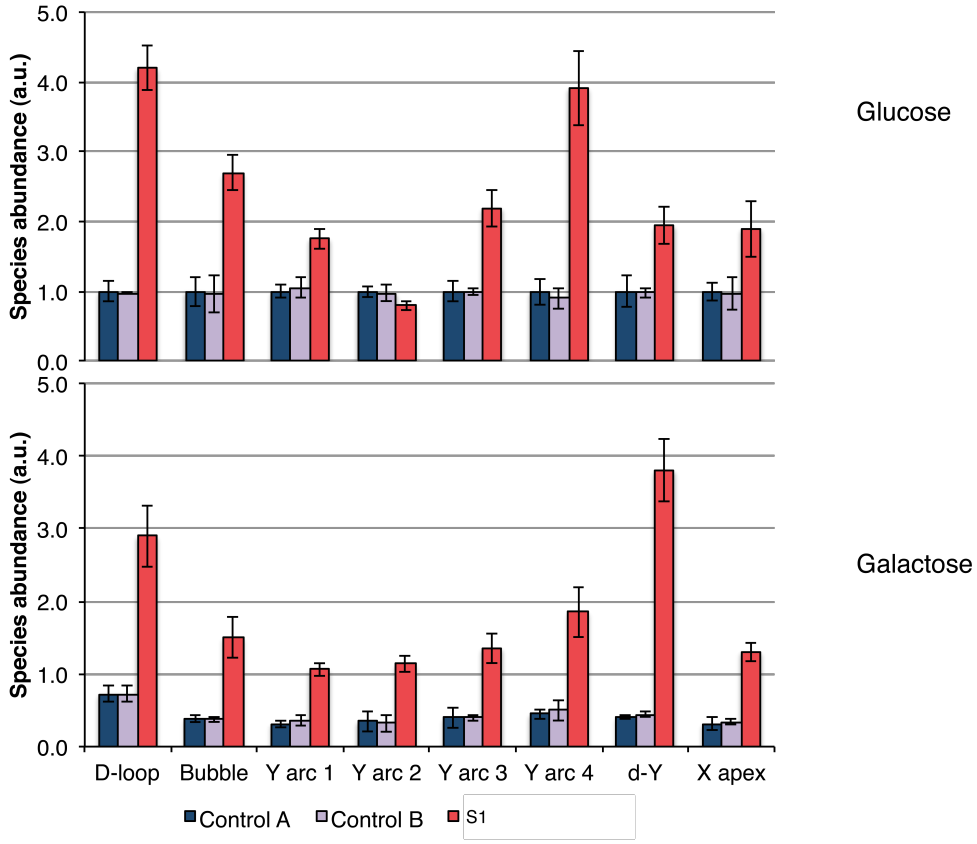

Replication intermediates and non-replicating mtDNA (1n) from cells growing in glucose or galactose for five days and shown in **Figure 2A** were quantified using ImageQuant software and normalized to the amount of non-replicating molecules (1n) for each sample. Control cells grown in glucose were arbitrarily chosen as reference and given value 1. ***$P < 0.001$; two-tailed unpaired Student's t test; $n = 2$; error bars = 1 s.d.

Table S1: Functional variants number filtered by public databases. The functions of variants include missense, readthrough, nonsense, spliceSite, 5'-UTR and 3'-UTR.

Filter method	**Functional variants (SNP+InDel)***
Before filtering	18,014+1,826
Filtered by 1000 Genome variants database	1,808+519
Filtered by 1000 Genome variants database_ HapMap	1,333+308
Filtered by 1000 Genome variants database_ HapMap_ESP	1,317+308

* SOAPaligner/SOAP2 (soap2.21) was use for mapping clean reads onto human reference genome (UCSC hg19, build 37.1), and SOAPsnp (v. 1.03) was used for SNP calling. BWA was used for mapping reads onto reference sequence in InDel analysis, and GATK (Genome Analysis Tool Kit) was used for InDel detection.

Table S2: Prioritization of candidate genes

Filter method	**Genes**
Recessive trait (≥2 variants/gene)	118
Only coding and splice-site variants	26
Predicted mitochondrial localization*	3 (*AGXT*, *RNASEH1*, *TIMM23*)

* Maestro score >0 (www.broadinstitute.org)

Table S3: *RNASEH1* mutations

Subject	DNA	Protein	Father/ Mother	Exac frequency	In vitro activity [a]	Mutation taster [b]	Polyphen2 [c]
S1	c.424G>A	p.Val142Ile	F	0.00004963	40%	Disease	Damaging
	c.469C>T	p.Arg157*	M	0.000008255	5%	Disease	/
S2	c.554C>T	p.Ala185Val	F	n.r.	20%	Disease	Damaging
	c.424G>A	p. Val142Ile	M	0.00004963	40%	Disease	Damaging
S3-6	c.424G>A	p. Val142Ile	F	0.00004963	40%	Disease	Damaging
	c.424G>A	p. Val142Ile	M	0.00004963	40%	Disease	Damaging

Nomenclature according to HGVS (NM_002936.4; NP_002927.2). F, father; M, mother. n.r.: not reported. [a]: compared to the activity of the wild-type enzyme.
[b]: http://www.mutationtaster.org (Disease= disease causing)
[c]: http://genetics.bwh.harvard.edu/pph2 (Damaging=probably damaging)